Supporting Information:

Fitting side-chain NMR relaxation data using molecular simulations

Felix Kümmerer,[†,§] Simone Orioli,[†,‡,§] David Harding-Larsen,[†] Falk Hoffmann,[¶,‖] Yulian Gavrilov,[†,⊥] Kaare Teilum,[†] and Kresten Lindorff-Larsen[*,†]

†*Structural Biology and NMR Laboratory, Linderstrøm-Lang Centre for Protein Science, Department of Biology, University of Copenhagen. Ole Maaløes Vej 5, DK-2200 Copenhagen N, Denmark*

‡*Structural Biophysics, Niels Bohr Institute, Faculty of Science, University of Copenhagen, Copenhagen, Denmark.*

¶*Theoretical Chemistry, Ruhr University Bochum, D-44780 Bochum, Germany*

§*Contributed equally to this work*

‖*Current address: Institute of Biomaterial Science and Berlin-Brandenburg Center of Regenerative Therapies, Helmholtz-Zentrum Geesthacht, Teltow, Germany*

⊥*Current address: Division of Biophysical Chemistry, Center for Molecular Protein Science, Department of Chemistry, Lund University, Lund, Sweden*

E-mail: lindorff@bio.ku.dk

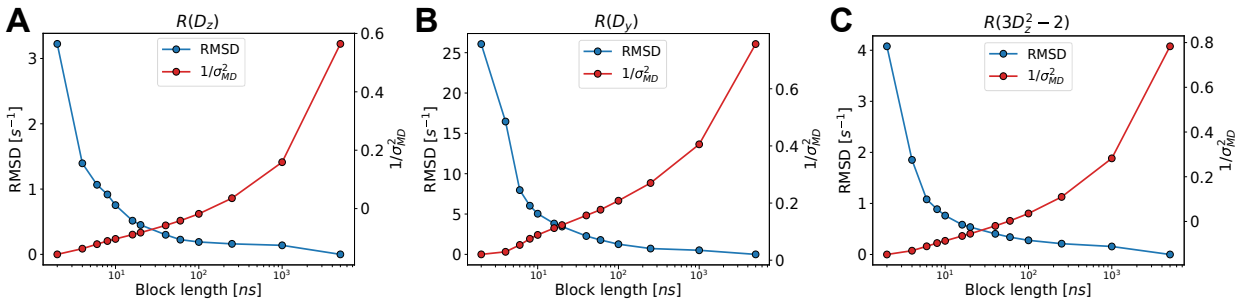

Figure S1: **Assessment of convergence and effect of block size.** RMSD of NMR relaxation rates (blue) and average inverse variance with respect to the full MD dataset (red) is shown as a function of the block length.

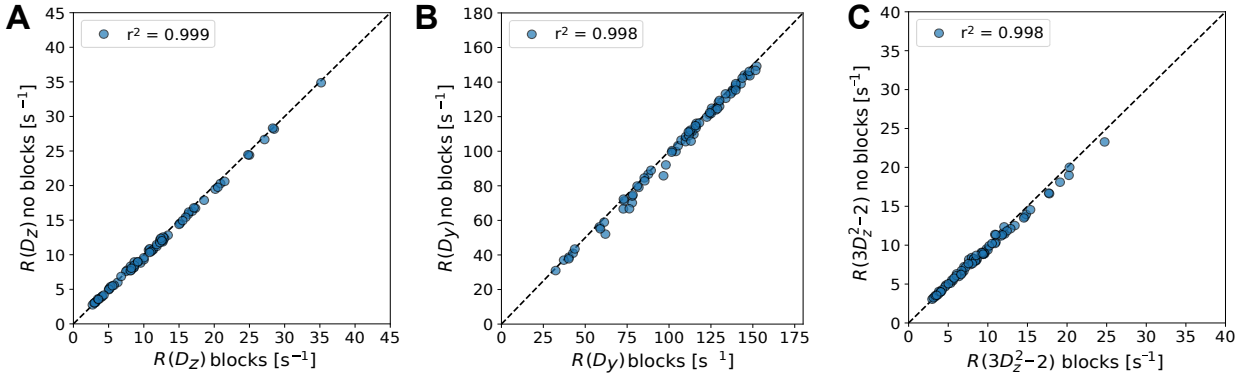

Figure S2: **Comparison of NMR relaxation rates calculated from 1500** 10 ns **blocks and the full MD dataset.** (A) $R(D_z)$, (B) $R(D_y)$ and (C) $R(3D_z^2-2)$ calculated from the MD dataset using 1500 10 ns long blocks and three 5 µs long blocks (no blocks). The label shows the corresponding Pearson correlation coefficient.

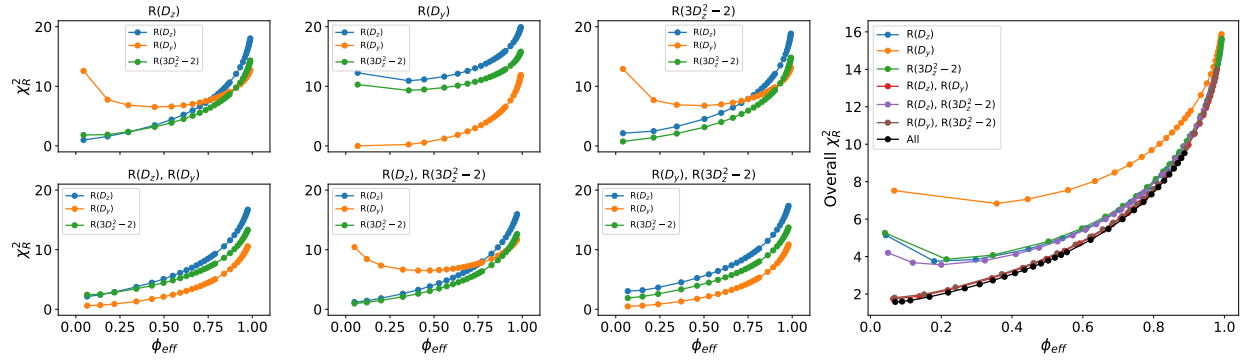

Figure S3: **Cross validation of ABSURDer reweighting when synthetic data were generated using the Amber ff99SB*-ILDN force field.** The panels show $\chi^2_R(\phi_{\text{eff}})$ curves for each of the three types of NMR relaxation rates. Each panel differs by which data was used in reweighting (label above panel), and we show the results using all six possible combinations of the three rates with the large panel corresponding to all three rates.

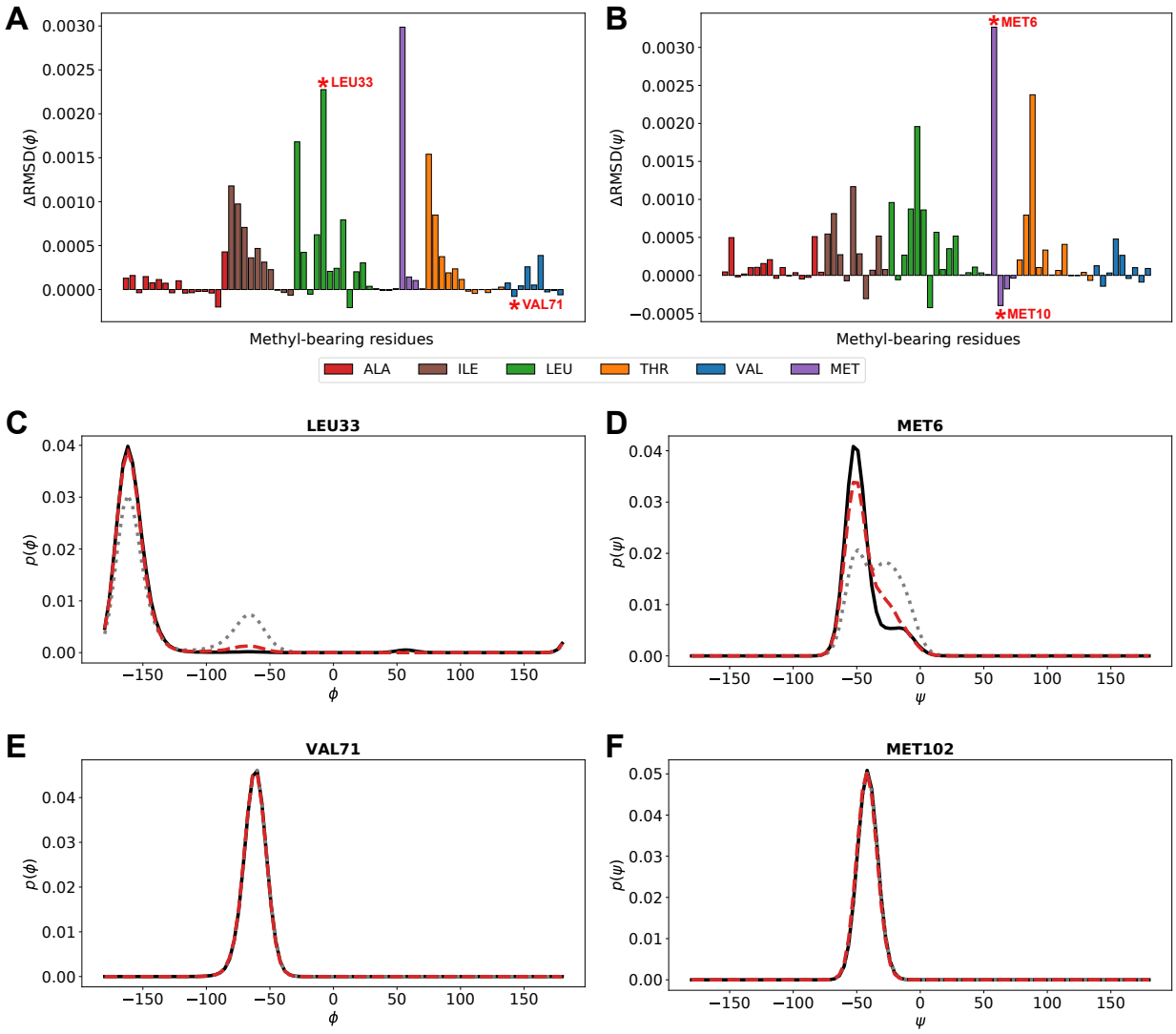

Figure S4: **Effect of ABSURDer reweighting on backbone dihedral angle distributions.** Difference RMSD (ΔRMSD) between distributions for the backbone (A) ϕ and (B) ψ dihedral angles. We calculated the RMSD of the dihedral angle distributions before (grey dotted line) and after (red dashed line) reweighting, in both cases using the distribution used to generate the synthetic data generated by Amber ff99SB*-ILDN as the reference (black solid line). Thus, large positive values of ΔRMSD indicate highly improved distributions after reweighting whereas negative values indicate distributions worsened by the application of ABSURDer. The bars are colored by residue type and asterisks mark residues highlighted in panels C–F. Examples of residues for which ABSURDer (C,D) substantially improve the dihedral angle distributions and (E,F) worsens them.

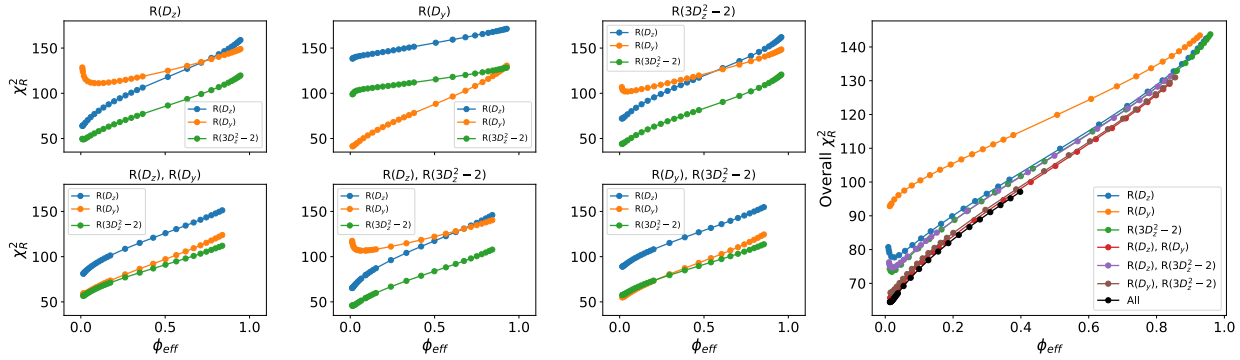

Figure S5: **Cross validation of ABSURDer reweighting when synthetic data were generated using the Amber ff15ipq force field.** The panels show $\chi^2_R(\phi_{\text{eff}})$ curves for each of the three types of NMR relaxation rates. Each panel differs by which data was used in reweighting (label above panel), and we show the results using all six possible combinations of the three rates with the large panel corresponding to all three rates.

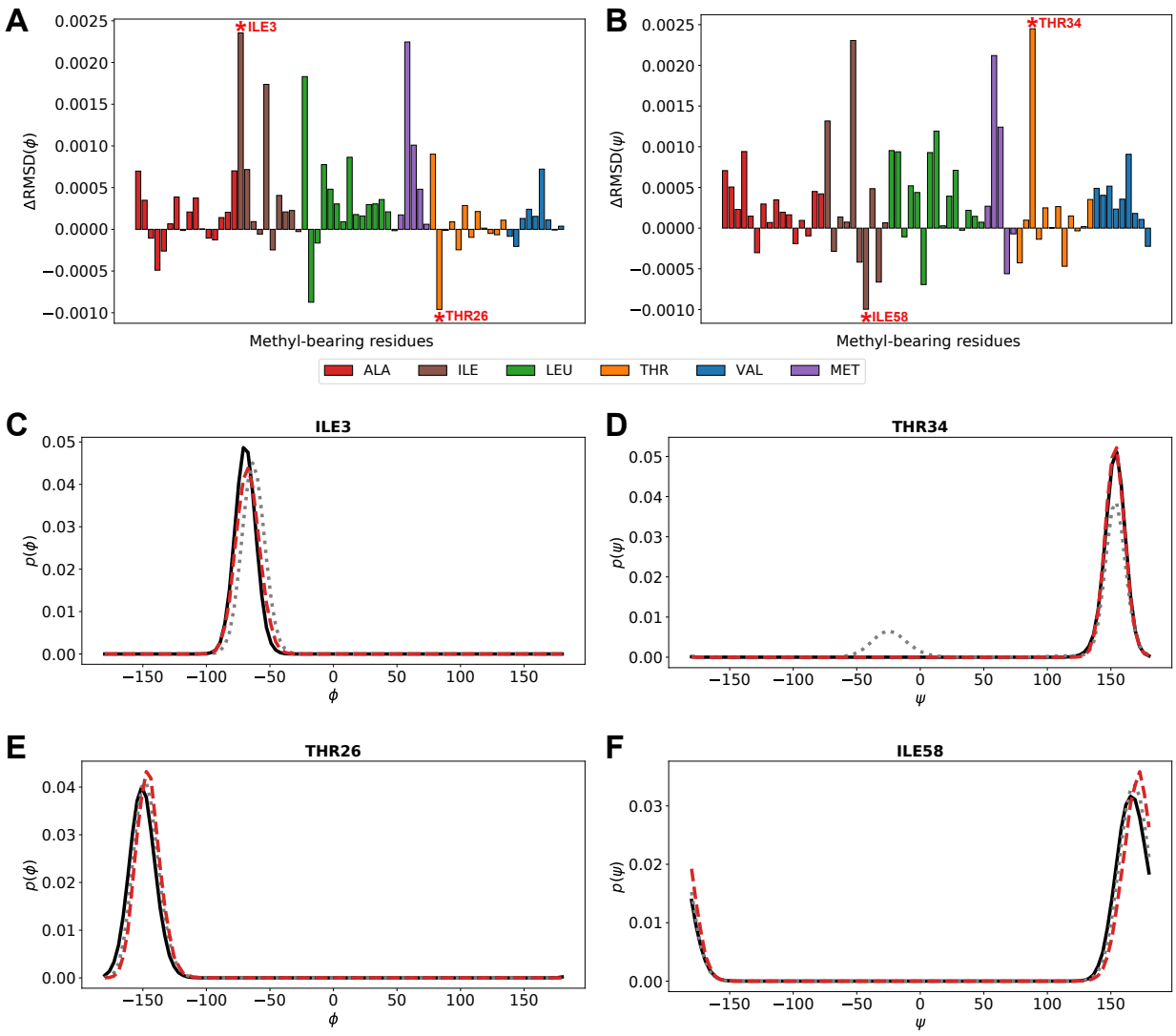

Figure S6: **Effect of ABSURDer reweighting on backbone dihedral angle distributions.** Difference RMSD (ΔRMSD) between distributions for the backbone (A) ϕ and (B) ψ dihedral angles. We calculated the RMSD of the dihedral angle distributions before (grey dotted line) and after (red dashed line) reweighting, in both cases using the distribution used to generate the synthetic data generated by Amber ff15ipq as the reference (black solid line). Thus, large positive values of ΔRMSD indicate highly improved distributions after reweighting whereas negative values indicate distributions worsened by the application of ABSURDer. The bars are colored by residue type and asterisks mark residues highlighted in panels C–F. Examples of residues for which ABSURDer (C,D) substantially improve the dihedral angle distributions and (E,F) worsens them.

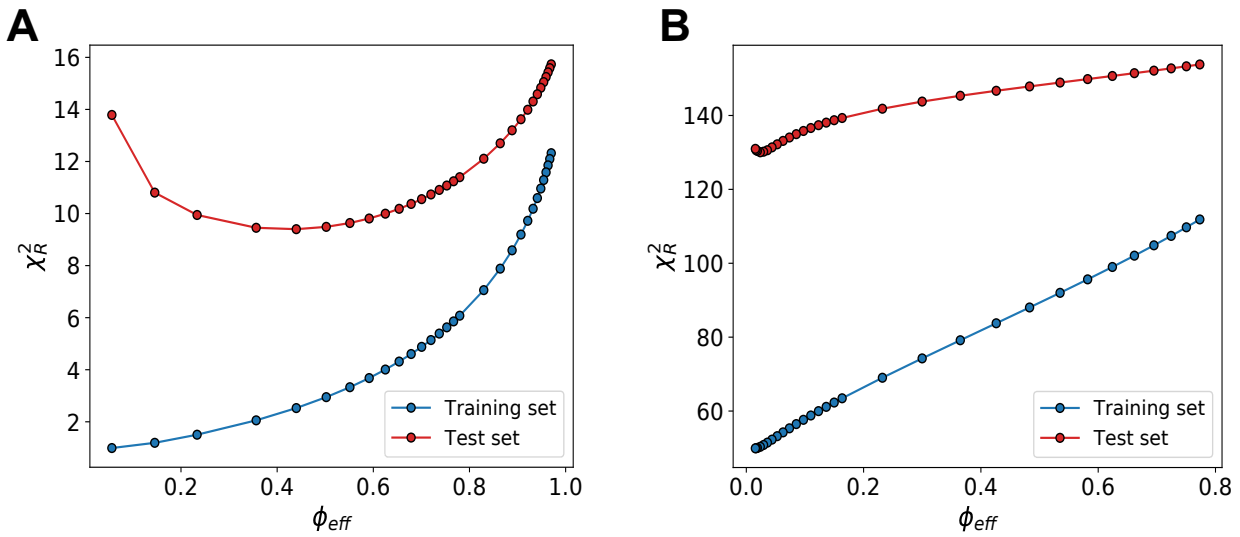

Figure S7: **Effect of ABSURDer reweighting on NMR relaxation rates not included in the optimisation**. We used ABSURDer with synthetic data to fit the relaxation rates for the (blue) 73 methyl groups that have been probed experimentally, and (red) cross-validate across the remaining 27 methyl groups. (A) Synthetic data generated with Amber ff99SB*-ILDN. (B) Synthetic data generated with Amber ff15ipq.

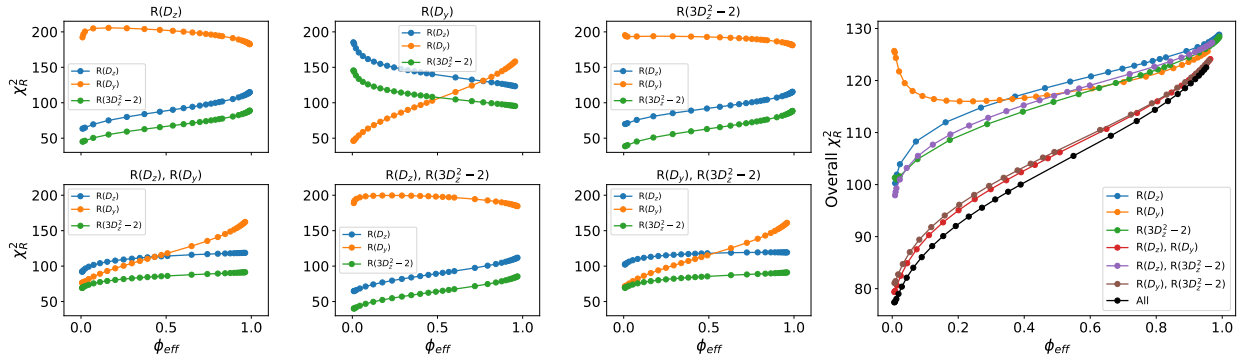

Figure S8: **Effect of ABSURDer reweighting on experimental data when only a subset of NMR relaxation rate types are used**. $\chi^2_R(\phi_{\text{eff}})$ curves for the three kinds of rate separately obtained by fitting with respect to all the possible combinations of rate types (6 panels on the left) and the corresponding average (overall χ^2_R, right panel).

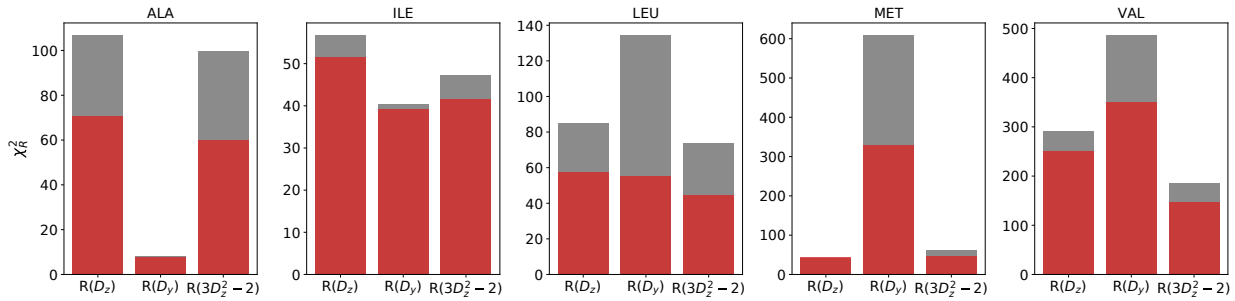

Figure S9: **Effect of ABSURDer on the different residue types**. Residue specific χ^2_R between calculated and experimental NMR relaxation rates before (grey) and after (red) reweighting. The results are obtained by averaging the residuals over the 15 ALA, 20 ILE, 5 MET, 14 VAL and 20 LEU residues. Note that each panel uses different scales for χ^2_R.

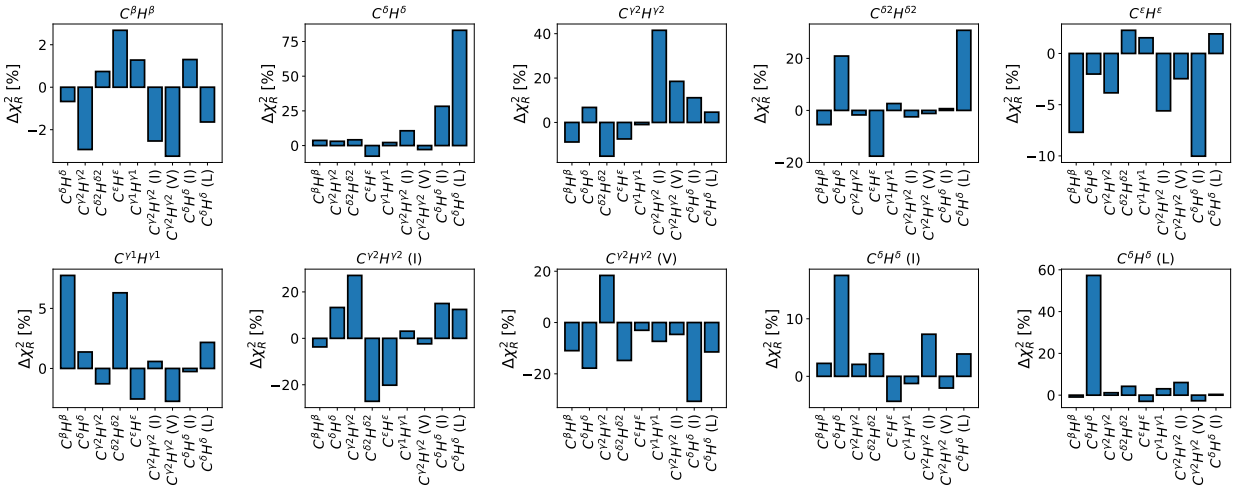

Figure S10: **Result of ABSURDer reweighting on NMR relaxation rates that were not included in the optimisation of specific methyl subsets**. We used ABSURDer to fit the relaxation rates for each methyl type separately and cross validated the results against the remaining methyl subsets. The y-axis reports the relative change in χ^2_R after the reweighting has been carried out on the methyl class specified in the plot titles. Negative values indicate that the agreement with experiments decreased, while positive values indicate improved agreement. Methyl types that are present across different types of residues are also shown separately (i.e. I, L and V).

Table S1: **Sum of the weights for blocks in each of the three independent** 5 µs **long trajectories.**

	Trajectory 1	**Trajectory 2**	**Trajectory 3**
Same force fields	0.21	0.5	0.29
Different force fields	0.28	0.45	0.27
Experimental	0.38	0.28	0.34